Available online at www.sciencedirect.com

SciVerse ScienceDirect

Current Opinion in Chemical Biology

# Label-free optical imaging of nonfluorescent molecules by stimulated radiation

Wei Min

Imaging contrasts other than fluorescence are highly desirable for label-free detection and interrogation of nonfluorescent molecular species inside live cells, tissues, and organisms. The recently developed stimulated Raman scattering (SRS) and stimulated emission microscopy techniques provide sensitive and specific contrast mechanisms for nonfluorescent species, by employing the light amplification aspect of stimulated radiation. Compared to their spontaneous counterparts, stimulated radiation can enhance the imaging performance significantly, making the previously 'dark' molecules observable. Here we review and summarize the underlying principles of this emerging class of molecular imaging techniques.

**Address**
Department of Chemistry, Columbia University, New York, NY 10027, United States

Corresponding author: Min, Wei (wm2256@columbia.edu)

**Current Opinion in Chemical Biology** 2011, **15**:831–837

This review comes from a themed issue on
Molecular Imaging
Edited by Alanna Schepartz and Ruben L Gonzalez, Jr.

Available online 4th November 2011

1367-5931/$ – see front matter


**DOI** 10.1016/j.cbpa.2011.10.005

## Introduction

Fluorescence microscopy is currently the most popular and powerful imaging technique used in biological studies [1]. This is mainly because of the unprecedented sensitivity offered by background-free fluorescence detection, and the exquisite labeling specificity thanks to genetically encoded fluorescent proteins [2–4], exogenous fluorophore dyes, and nanocrystals [5]. As such, various versatile fluorescence-based imaging techniques, such as confocal laser scanning [1], two-photon excited fluorescence [6], single-molecule microscopy [7,8], and super resolution imaging [9,10], have flourished and greatly advanced modern life sciences.

However, fluorescence microscopy faces two fundamental limitations. First, many intracellular small molecules such as metabolites, signaling peptides, neurotransmitters, and drugs are intrinsically nonfluorescent. It is no longer feasible to label these small molecules with fluorescent labels, because the exogenous labels are larger than the sizes of the small molecules of interest. Second, many intracellular chromophores such as hemoglobin and cytochromes absorb light but do not fluoresce efficiently, due to their fast nonradiative decay rates from excited states. Imaging the distributions of nonfluorescent small molecules and chromophores with high sensitivity using novel optical contrasts is a nontrivial task.

Hence, optical imaging methods other than fluorescence will be highly desirable in biomedical sciences and applications. To this end, two different but related optical imaging techniques have been recently developed to cope with the two challenges: stimulated Raman scattering microscopy for imaging small chemical species, and stimulated emission microscopy for imaging chromophores with nondetectable fluorescence. Spectroscopically, both of them take advantage of the light amplification aspect of stimulated radiation which includes both the scattering and the emission processes. By directly interrogating vibrational and electronic energy levels of molecules, respectively, they offer contrast mechanisms for label-free molecular imaging with high sensitivity and specificity.

## Stimulated Raman scattering microscopy

Raman spectroscopy, which disperses and detects inelastic scattering of incident photons off Raman-active molecular vibrations, offers label-free contrast based on characteristic vibrational frequencies for all major biochemical species, such as lipids, water, DNA, and proteins, as well as a variety of small molecules such as drugs or metabolites [11]. Figure 1 summarizes various Raman interactions. Unfortunately, the spontaneous Raman cross-sections are typically 10–12 orders of magnitudes smaller than the absorption/fluorescence cross-sections. As a result, very long acquisition times are often required for spontaneous Raman microscopy [11]. In addition, the auto-fluorescence background of biological specimen often overwhelms the feeble spontaneous Raman signal from the target species.

Coherent anti-Stokes Raman scattering (CARS), which makes use of the coherent amplification excited by joint pump and Stokes beams, drastically increases the otherwise weak Raman scattering signal [12–14]. CARS has been applied to fast imaging of biological samples since 1999 [15•]. However, CARS microscopy suffers from spectral distortion, limited sensitivity arising from an unwanted nonresonant background, nonlinear concentration dependence, and coherent image artifacts [12–14,15•]. Special CARS derivatives exist to alleviate some of these difficulties, but they normally involve much increased complexity of instrumentation and data extraction.

**Figure 1**

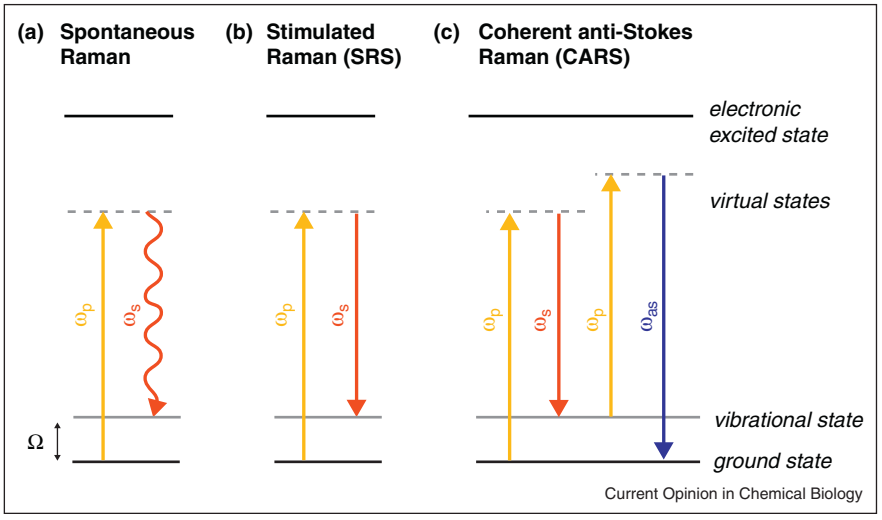


Energy diagram of various Raman interactions. **(a)** Spontaneous Raman scattering. Pump field is inelastically scattered off molecular vibrations, generating new and red-shifted field components at the Stokes frequencies $\omega_s = \omega_p - \Omega$. **(b)** Stimulated Raman scattering (SRS). Both Pump and Stokes frequencies are provided to illuminate the sample. When the frequency difference $\omega_p - \omega_s$ matches a molecular vibration, $\Omega$, stimulated excitation of the vibration transition occurs. **(c)** Coherent anti-Stokes Raman scattering (CARS). CARS is a four-wave mixing process generating a new field at the anti-Stokes frequency $\omega_{as} = 2\omega_p - \omega_s$. When the energy difference between $\omega_p$ and $\omega_s$ matches a molecular vibration, the scattering process is resonantly enhanced.

Historically, the stimulated Raman scattering (SRS) effect was discovered immediately after the laser was invented [16•,17,18•]. Since then, stimulated Raman spectroscopy has been performed on various molecular systems [19–21]. In particular, femtosecond stimulated Raman spectroscopy provides vibrational structural information of chromophores with both high temporal and spectral resolution [22]. In terms of imaging applications, SRS as a contrast mechanism for microscopy was first reported in 2007 using multiplex detection combined with a femtosecond amplified laser system [23•]. However, the amplified laser system is not suitable for bio-imaging because of the excessive peak power and the low repetition rate. This problem was overcome by using narrow-band high-repetition-rate picosecond pulse trains and high-frequency modulation transfer, which yielded superior sensitivity and fast imaging speed. This new, rapid, and sensitive SRS microscopy was first demonstrated by Xie and coworkers in 2008 [24••], followed immediately by independent reports from two other groups [25,26].

As opposed to CARS which probes vibrational coherence by detecting the anti-Stokes radiation, SRS probes the excited vibrational population through a gain or loss detection of the incident beams [12]. As shown in Figure 2, when the energy difference ($\Omega$) between the input pump and Stokes beams is tuned into a vibrational resonance frequency, $\Omega \rightarrow \omega_v$, the rate of the vibrational excitation will be greatly accelerated compared to that in spontaneous Raman by a factor of $r_{stim.Raman}/r_{spon.Raman} = n_{probe} + 1$, where $n_{probe}$ is the (normally large) number of photons in the optical mode of the probe beam [14,18]. As required by energy conservation, each quantum of the vibrational excitation is accompanied by one photon being annihilated from the pump beam and simultaneously a photon being created into the Stokes beam. The resulting intensity loss in the pump beam and the intensity gain in the Stokes beam, which is called stimulated Raman loss and stimulated Raman gain, respectively, are the optical signals of SRS.

In a typical SRS bio-imaging setup, two temporally synchronized ultrafast pump and Stokes pulse trains are spatially combined and focused collinearly onto a common focal spot. Before the sample, the intensity of the Stokes beam is modulated at a high frequency $f$ (>5 MHz), while the pump beam is originally un-modulated. After interacting with the sample, only the intensity of the pump beam is collected and detected by a photodiode. The readout of the photodiode is then demodulated by a lock-in amplifier to extract the modulation depth at the frequency $f$. When the Stokes beam is blocked, the pump beam maintains its intensity after passing through the sample; when the Stokes beam is unblocked, the pump beam experiences stimulated Raman loss in the vibrationally resonant condition. Hence, a temporal modulation of the Stokes beam at $f$ would give rise to a modulation of the transmitted pump beam intensity, at the same frequency $f$. Such a high-frequency modulation signal can be sensitively detected

**Figure 2**

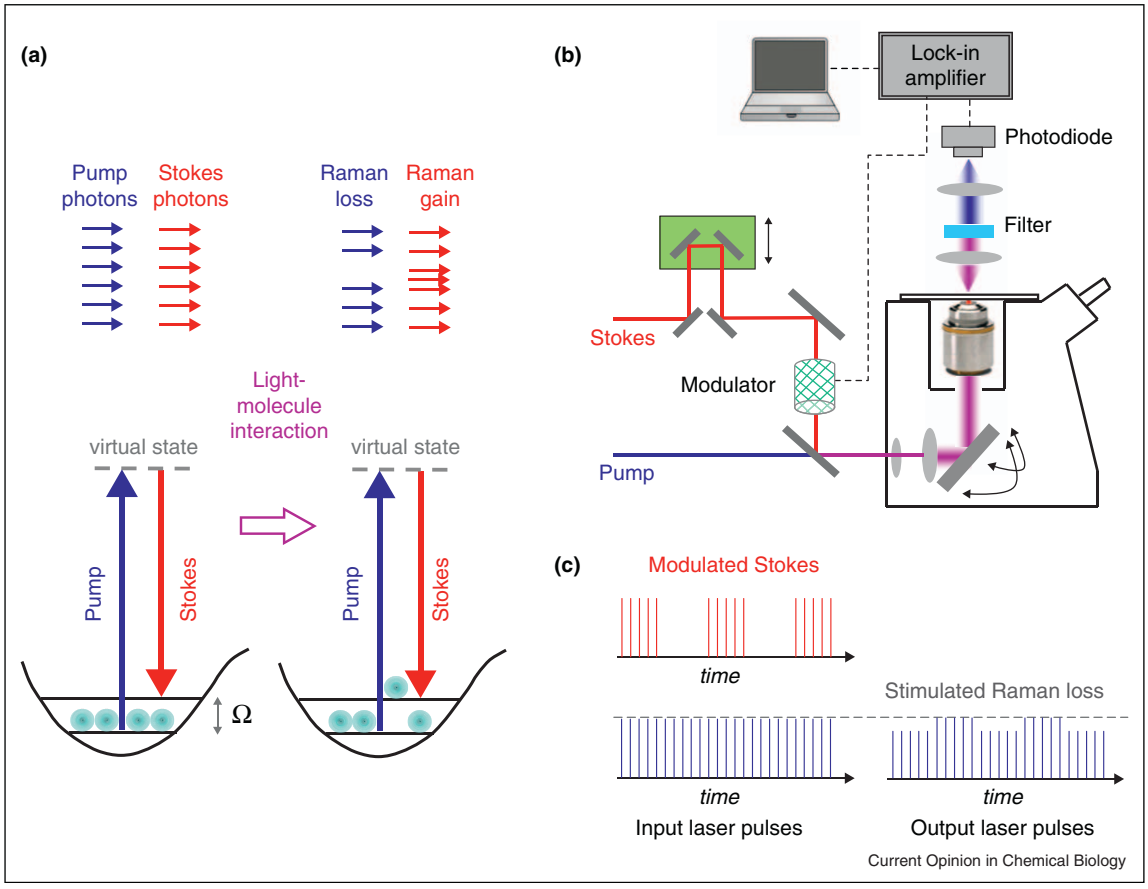


Principle of SRS microscopy. **(a)** Energy diagram of SRS when the energy difference between the synchronized Pump and Stokes beams is resonant with the vibrational level, of a particular chemical bond. As a result of the joint action between the Pump and Stokes beams, the vibrational excitation is greatly accelerated compared to that of spontaneous Raman. Meanwhile, optical energy will transfer from the Pump beam to the Stokes beam to power the vibrational excitation and to fulfill energy conservation. Consequently, the Stokes beam and the Pump beam exhibit stimulated Raman gain and stimulated Raman loss, respectively. **(b)** SRS microscope. A fast modulation scheme is utilized to remove slow laser noise. The intensity of the Stokes beam is modulated at ~10 MHz by a modulator, and the transmitted Pump beam is detected by a photodiode and then demodulated by a lock-in amplifier. **(c)** Temporal modulation of the input and output Pump and Stokes pulse trains. The stimulated Raman loss signal is highlighted as a periodic intensity modulation.

above the laser intensity noise. With the amount of the modulation transfer being registered for each pixel, a three-dimensional (3D) image is then constructed by scanning the combined pump/Stokes laser beams across the sample point-by-point with a scanning microscope.

It is the optical amplification of the vibrational excitation rate that lies in the orders of magnitude enhancement of the SRS imaging speed over that of spontaneous Raman microscopy. A 5 mM methanol solution ($\sim 3 \times 10^5$ C–H bonds within the focal volume) gives a stimulated Raman loss signal of about $\Delta I_{SRS}/I_p \sim 7 \times 10^{-8}$ [24]. With a known $\sigma_{Raman} \sim 10^{-29}$ cm$^2$ for one C–H bond, the total spontaneous Raman scattering cross-sections of $3 \times 10^5$ bonds will add up to a cross-section of $3 \times 10^{-24}$ cm$^2$. Given a laser waist area of $10^{-9}$ cm$^2$, one would expect to produce a relative spontaneous Raman signal of $\Delta I_{spon.Raman}/I_p = (3 \times 10^{-24}\ cm^2)/(10^{-9}\ cm^2)–3 \times 10^{-15}$. Therefore, $r_{stim.Raman}/r_{spon.Raman}$ is estimated to be $7 \times 10^{-8}/3 \times 10^{-15}–10^7$, an enhancement large enough for applications such as *in vivo* video-rate SRS microscopy of live animals becomes feasible [27].

As a chemical imaging technique superseding CARS, SRS microscopy exhibits a number of favorable properties [28••]. First, SRS is free from the nonresonant background. This is so because, in the absence of a vibrational eigenstate that could hold the population, energy simply cannot transfer from the pump beam to the Stokes beam, as required by energy conservation. Second, without the interference effect from the background, the SRS spectrum is identical to that of spontaneous Raman scattering.

**Figure 3**

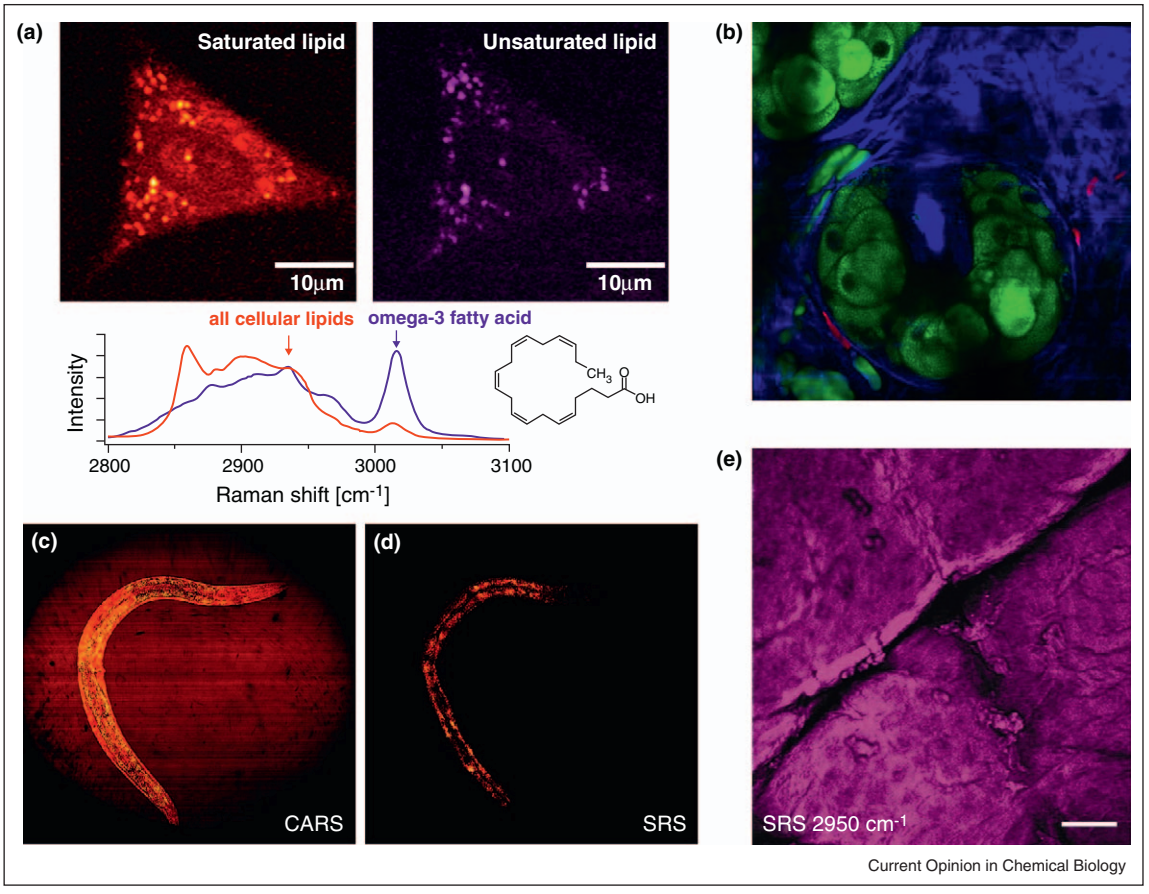


SRS imaging in cells, tissues, organisms and humans. **(a)** Saturated and unsaturated fatty acid images of a lung cancer cell incubated with ω−3 fatty acids, adapted from Ref. [24••]. The strong peak at 3015 $cm^{-1}$ is characteristic of unsaturated fatty acids. **(b)** Lipid (*green*) and protein (*blue*) images of a sebaceous gland of mouse skin showing lipid-rich gland cells and adipocytes as well as protein-rich structures such as hairs and collagen. Overlaid are micro-capillaries due to red blood cells (*magenta*). Simultaneous **(c)** CARS and **(d)** SRS lipid images of a live worm, *C. elegans*. Whereas SRS specifically probes lipid contributions, CARS is complicated by the nonresonant background. **(e)** SRS image of the stratum corneum on a human skin surface tuned into the $CH_3$ stretching of proteins (2950 $cm^{-1}$).
Adapted from Ref. [27].

Third, the detection sensitivity of SRS is much higher than that of CARS microscopy. Thanks to the high-frequency modulation at a high $f$, SRS can detect $\Delta I_p/I_p$ of $10^{-8}$ within 1 s. Fourth, the strict linear concentration dependence of SRS permits straightforward and reliable quantification. Fifth, as SRS is automatically phase matched, there exists a well-defined point spread function that can be used for image deconvolution.

Having achieved label-free vibrational specificity, unprecedented imaging speed and superb detection sensitivity, SRS has opened up a wide range of chemical imaging applications by targeting various vibrational bands, as highlighted in Figure 3. For example, unlike CARS microscopy, SRS only probes the lipid contribution from the intestine and the hypodermal skin of *Caenorhabditis elegans* without the nonresonant background contribution from other tissues, representing a major advantage for *in vivo* lipid analysis [29,30]. When combined with powerful genetic manipulations (RNA interference, in particular) of this model organism, the underlying genes responsible for lipid storage and distribution can be screened and identified in a high-throughput manner [29].

## Stimulated emission microscopy

Stimulated emission was first proposed by Einstein in 1917 and later confirmed experimentally in 1928. An atom or molecule in its excited electronic state can be stimulated down to the ground state by an incident photon with the appropriate frequency, resulting in the creation of a new coherent photon identical to the original incident one in all physical aspects including energy, polarization, and phase. Population de-excitation of the molecular excited state and the optical amplification of the incident

**Figure 4**

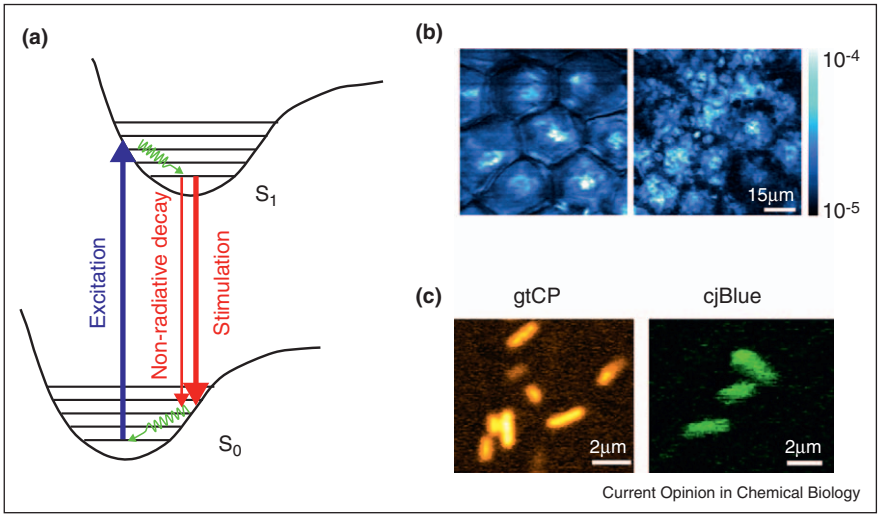


Stimulated emission microscopy. **(a)** Energy diagram of stimulated emission followed by optical excitation, when applied to nonfluorescent chromophores. As the chromophore is cycling between the electronic states driven by the pulsed excitation beam and the pulsed stimulation beam at the right timing, the stimulation beam will gain intensity, which can be detected with a high sensitivity. **(b)** A pair of stimulated emission images of toluidine blue O, a drug used as photosensitizer in photodynamic therapy, at two different *z*-depths (3 and 25 μm, respectively), delivered onto a mouse ear. Optical sectioning is evident. **(c)** Stimulated emission images of genetically encoded nonfluorescent chromoproteins, gtCP, and cjBlue, respectively, inside *Escherichia coli* cells that contain corresponding expression plasmids.
Images adapted from Ref. [33••].

beam are the two sides of the same coin for stimulated emission. The population dumping aspect has been utilized in optical microscopy, such as in stimulated emission depletion for super resolution fluorescence imaging [9,31] and in fluorescence lifetime imaging [32]. On the other hand, the optical amplification process of the incident field, which is precisely the working principle for the laser, has rarely been used for microscopy.

The light amplification aspect of stimulated emission is the underlying principle of stimulated emission microscopy which is designed for highly sensitive imaging of nonfluorescent chromophores [33••], summarized in Figure 4. Many chromophores, such as hemoglobin and cytochromes, absorb light intensely but have undetectable fluorescence. This is so because their spontaneous emission is dominated by their fast nonradiative decay (which can be four orders of magnitude faster than their rate of spontaneous emission) from the excited state. With the introduction of a stimulation pulse with appropriate time delay and energy, the chromophore, after being photoexcited to the excited state by an excitation pulse, is much more likely to be brought down to the ground state through the radiative decay channel (which is now enhanced by the presence of a strong stimulation beam) compared to the nonradiative decay channel. As a result of the new photons radiated by the molecule, the intensity of the stimulation beam is concurrently increased. Such an intensity gain can be extracted by a high-frequency modulation scheme (the same detection method used in SRS), making the chromophore detectable. In some sense, the previously dark chromophore molecule is now forced to emit light in the form of stimulated emission.

The excitation beam and the stimulation beam have to be in the form of ultrashort pulse trains to effectively interrogate the transient excited states, as the excited lifetimes of those nonfluorescent chromophores are extremely brief (less than one picosecond). In addition, the excitation pulse train and the stimulation pulse train do not need to overlap in time. In fact, the stimulation pulse train is delayed by a few hundred femtoseconds with respect to the excitation pulse train, to permit the molecule enough time to relax vibrationally on the electronic excited state. This delay is also useful to separate the stimulated emission from other instantaneous processes such as SRS or cross-phase modulation.

Stimulated emission microscopy, which is highly related to absorption imaging, exhibits a few advantages over direct one-beam absorption microscopy. First, the stimulated emission signal is only generated at the laser spot, offering 3D optical sectioning. Second, the high-frequency modulation transfer scheme provides shot-noise limited detection sensitivity, while one-beam absorption suffers from laser intensity noise at low frequencies. Third, the absorption approach cannot distinguish true optical absorption from light scattering from heterogeneous biological samples, as both effects are manifested as light extinction. In contrast, stimulated emission microscopy measures the

response of the stimulation beam intensity only at the modulation frequency, filtering out the sample scattering effect at low frequencies.

## Concluding remarks

It is constructive to summarize the common strategy employed by both stimulated Raman scattering microscopy and stimulated emission microscopy. When the spontaneous Raman scattering is too weak for typical vibrational oscillators, stimulated Raman is used to significantly boost the vibrational excitation rate, imaging speed, and sensitivity. Likewise, when the spontaneous emission (i.e. fluorescence) is too weak for nonfluorescent chromophores, stimulated emission is used to enhance the radiative decay rate. Hence, stimulated radiation can indeed improve on the imaging performance of its spontaneous counterpart.

The detection sensitivity of both stimulated Raman scattering microscopy and stimulated emission microscopy has approached the shot-noise limit of the incident laser beam, which arises from stochastic arrivals of photons at the detector. This poses a fundamental challenge as to how to further improve the sensitivity to study even more dilute molecular species. We envision that the principles and techniques from quantum optics, such as entangled photons and squeezed light, might be borrowed to create a 'quantum jump' for the detection sensitivity beyond the shot-noise limit.

While the chemical biology strategies of fluorescence labeling have become increasingly sophisticated [34,35], many more molecular species cannot or should not be labeled in biomedical applications. To this end, stimulated Raman scattering microscopy and stimulated emission microscopy represent an emerging direction for nonfluorescent optical imaging. Exciting applications in various areas are expected for many years to come.

## Acknowledgements

We are grateful to X. Sunney Xie and the members of his group who have contributed to the development and applications of stimulated Raman scattering microscopy and stimulated emission microscopy, in particular, C.W. Freudiger, S. Lu, B.G. Saar, S. Chong, G.R. Holtom, M. Roeffaers, X. Zhang and R. Roy. In addition, we wish to thank M.C. Wang, J.X. Kang and G. Ruvkun for collaboration on lipid biology.

## References and recommended reading

Papers of particular interest, published within the period of review, have been highlighted as:

- • of special interest
- •• of outstanding interest

1. Pawley JB (Ed): *Handbook of Biological Confocal Microscopy*, edn 3. Springer; 2006.

2. Chalfie M, Tu Y, Euskirchen G, Ward WW, Prasher DC: **Green fluorescent protein as a marker for gene expression**. *Science* 1994, **263**:802-805.

3. Tsien RY: **The green fluorescent protein**. *Annu Rev Biochem* 1998, **67**:509-544.

4. Zhang J, Campbell RE, Ting AY, Tsien RY: **Creating new fluorescent probes for cell biology**. *Nat Rev Mol Biol* 2002, **3**:906-918.

5. Michalet X, Pinaud FF, Bentolila LA, Tsay JM, Doose S, Li JJ, Sundaresan G, Wu AM, Gambhir SS, Weiss S: **Quantum dots for live cells, *in vivo* imaging, and diagnostics**. *Science* 2005, **307**:538-544.

6. Denk W, Strickler J, Webb WW: **Two-photon laser scanning fluorescence microscopy**. *Science* 1990, **248**:73-76.

7. Moerner WE, Orrit M: **Illuminating single molecules in condensed matter**. *Science* 1999, **283**:1670-1676.

8. Xie XS, Trautman JK: **Optical studies of single molecules at room temperature**. *Annu Rev Phys Chem* 1998, **49**:441-480.

9. Hell SW: **Far-field optical nanoscopy**. *Science* 2007, **316**:1153-1158.

10. Huang B, Babcock H, Zhuang X: **Breaking the diffraction barrier: super-resolution imaging of cells**. *Cell* 2010, **143**:1047-1058.

11. Turrell G, Corset J: *Raman Microscopy: Developments and Applications*. San Diego: Academic Press; 1996.

12. Levenson MD, Kano SS: *Introduction to Nonlinear Laser Spectroscopy*. San Diego: Academic Press; 1988.

13. Clark RJH, Hester RE (Eds): *Advances in Nonlinear Spectroscopy*, vol 15. New York: John Wiley and Sons Ltd.; 1988.

14. Boyd RW: *Nonlinear Optics*. London: Academic; 2003.

15. • Zumbusch A, Holtom GR, Xie XS: **Three-dimensional vibrational imaging by coherent anti-Stokes Raman scattering**. *Phys Rev Lett* 1999, **82**:4142-4145.
The modern version of coherent anti-Stokes Raman scattering microscopy is presented.

16. • Woodbury EJ, Ng WK: **Proc Inst Radio Eng**1962, **50**:2347-2348.
The very first report of stimulated Raman scattering effect.

17. Jones WJ, Stoicheff BP: **Inverse Raman spectra: induced absorption at optical frequencies**. *Phys Rev Lett* 1964, **13**:657-659.

18. • Bloembergen N: **The stimulated Raman effect**. *Am J Phys* 1967, **35**:989-1023.
The first systematic theoretical treatment of stimulated Raman scattering effect.

19. Owyoung A: **Coherent Raman gain spectroscopy using CW laser sources**. *IEEE J Quant Electron* 1978, **QE-14**:192-203.

20. Levine BF, Shank CV, Heritage JP: **Surface vibrational spectroscopy using stimulated Raman scattering**. *IEEE J Quant Electron* 1979, **QE-15**:1418-1432.

21. Levenson MD, Moerner WE, Horne DE: **FM spectroscopy detection of stimulated Raman gain**. *Opt Lett* 1983, **8**:108-110.

22. Kukura P, McCamant DW, Mathies RA: **Femtosecond stimulated Raman spectroscopy**. *Annu Rev Phys Chem* 2007, **58**:461-488.

23. • Ploetz E, Laimgruber S, Berner S, Zinth W, Gilch P: **Femtosecond stimulated Raman microscopy**. *Appl Phys B* 2007, **87**:389-393.
Stimulated Raman scattering as a contrast mechanism is demonstrated with femtosecond amplified laser system together with multiplex detection.

24. •• Freudiger CW, Min W, Saar BG, Lu S, Holtom GR, He C, Tsai JC, Kang JX, Xie XS: **Label-free biomedical imaging with high sensitivity by stimulated Raman scattering microscopy**. *Science* 2008, **322**:1857-1861.
The first demonstration of stimulated Raman scattering microscopy using narrow-band high-repetition-rate picosecond pulse trains and high-frequency modulation transfer, which yielded superior sensitivity and fast imaging speed.

25. Nandakumar P, Kovalev A, Volkmer A: **Vibrational imaging based on stimulated Raman scattering microscopy**. *New J Phys* 2009, **11**:033026-33035.

26. Ozeki Y, Dake F, Kajiyama S, Fukui K, Itoh K: **Analysis and experimental assessment of the sensitivity of stimulated Raman scattering microscopy**. *Opt Express* 2009, **17**:3651-3658.

27. Saar BG, Freudiger CW, Reichman J, Stanley MC, Holtom GR, Xie XS: **Video-rate molecular imaging *in vivo* with stimulated Raman scattering**. *Science* 2010, **330**:1368-1370.

28. •• Min W, Freudiger CW, Lu S, Xie XS: **Coherent nonlinear optical imaging: beyond fluorescence microscopy**. *Annu Rev Phys Chem* 2011, **62**:507-530.
A comprehensive and technical comparison between CARS and SRS microscopy is provided.

29. Wang MC, Min W, Freudiger CW, Ruvkun G, Xie XS: **RNAi screening for fat regulatory genes with SRS microscopy**. *Nat Methods* 2011, **8**:135-138.

30. Bewersdorf J, Farese RV, Walther TC: **A new way to look at fat**. *Nat Methods* 2011, **8**:132-133.

31. Hell SW, Wichmann J: **Breaking the diffraction resolution limit by stimulated emission: stimulated-emission-depletion fluorescence microscopy**. *Opt Lett* 1994, **19**:780-782.

32. Dong CY, So PT, French T, Gratton E: **Fluorescence lifetime imaging by asynchronous pump-probe microscopy**. *Biophys J* 1995, **69**:2234-2242.

33. •• Min W, Lu S, Chong S, Roy R, Holtom GR, Xie XS: **Imaging chromophores with undetectable fluorescence by stimulated emission microscopy**. *Nature* 2009, **461**:1105-1109.
Stimulated emission as a contrast mechanism for microscopy is first demonstrated.

34. Jing C, Cornish VW: **Chemical tags for labeling proteins inside living cells**. *Acc Chem Res* 2011, **44**:784-792.

35. Fernandez-Suarez M, Ting AY: **Fluorescent probes for super-resolution imaging in living cells**. *Nat Rev Mol Cell Biol* 2008, **9**:929-943.